Near-infrared Thermal Emission From The Hottest Of The Hot Jupiters

Bryce Croll (University of Toronto), Loic Albert (CFHT), Ray Jayawardhana (UofT), David Lafreniere (Universite de Montreal), Jonathan Fortney (UC Santa Cruz), Michael Cushing (JPL) , John A. Johnson (Caltech).

University of Toronto

Abstract: We have used the Wide-field Infrared Camera (WIRCam) on the Canada France Hawaii Telescope (CFHT) to detect thermal emission in the near-infrared from the hot Jupiters TrES-2b (Ks-band), TrES-3b (Ks-band and an H-band upper limit), WASP-3b (two Ks-band eclipses), and WASP-12b (a Ks, H & J-band eclipse). We discuss the implications of these detections below. We parameterize the level of redistribution from the day to nightside by the reradiation factor, f, following the Lopez-Morales & Seager (2007) definition, and note that the wavelengths of our near-infrared bands are centered at approximately 2.15 microns (Ks), 1.63 microns (H) and 1.25 microns (J).

1. TrES-2b:

We obtained photometry bracketing the secondary eclipse of the hot Jupiter TrES-2b in June 2009 using WIRCam on CFHT. We detected its thermal emission in Ks-band (Figure 1.1). Our eclipse detection is consistent with zero eccentricity. Our observations, when combined with recent Spitzer/IRAC observations of this planet (O'Donovan et al. 2009), can be fit by a wide range of Bond albedos and efficiencies of redistribution of heat from the day to nightside (Figure 1.3). If we assume a Bond albedo near zero, consistent with theoretical predictions and observations of other hot Jupiters, then TrES-3b is best-fit with a near isothermal dayside temperature profile, and very efficient redistribution of heat (Figure 1.4). This material is described in Croll et al. (submitted).

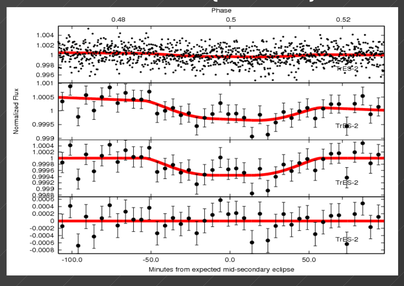

Figure 1.1: WIRCam/CFHT photometry bracketing the secondary eclipse of TrES-2b in Ks-band. The top panel shows the unbinned lightcurve, while the panel that is the second from the top shows the lightcurve with the data binned every 5 minutes. The panel that is the second from the bottom shows the binned data after the subtraction of the best-fit background, while the bottom panel shows the binned residuals from the best-fit model. In each one of the panels the best-fit best-fit secondary eclipse and background is shown with the red line.

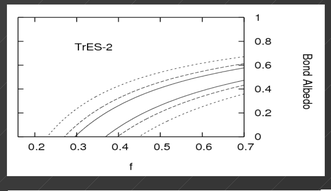

Figure 1.2: The 1-sigma (solid-line), 2-sigma (dashed-line), and 3-sigma (short dashed-line) chi-squared confidence regions on the reradiation factor, f, and Bond albedo from the combination of our Ks-band point and the Spitzer/IRAC measurements.

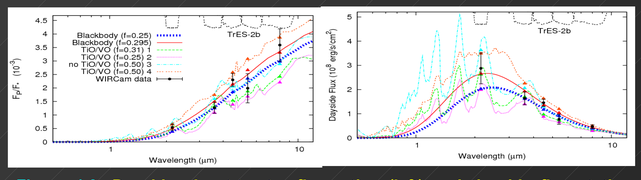

Figure 1.3: Dayside planet-to-star flux ratios (left) and dayside flux at the planet's surface (right). The Ks-band point (~2.15 microns) is our own, while the Spitzer/IRAC points are from O'Donovan et al. (2009). Blackbody curves for isotropic reradiation (f=1/4; blue dashed line) and our best-fit reradiation factor (f=0.32; red line) are also plotted. We also plot one-dimensional, radiative transfer spectral models (Fortney et al. 2006; 2008) for various reradiation factors and with and without TiO/VO. We plot the Ks-band WIRCam and Spitzer/IRAC transmission curves inverted at arbitrary scale at the top of both panels (dotted black lines).

2. TrES-3b:

We obtained photometry bracketing two secondary eclipses of the hot Jupiter TrES-3b in June 2009 using WIRCam on CFHT. We detected thermal emission from TrES-3b in Ks-band (Figure 2.1 left), but were unable to detect its emission in H-band (Figure 2.1 right). Our eclipse detection is consistent with zero eccentricity (Figure 2.2). Our observations, when combined with recent Spitzer/IRAC observations of this planet (Fressin et al. 2009), can be fit by a wide range of Bond albedos and efficiencies of redistribution of heat from the day to nightside (Figure 2.3). If we assume a Bond albedo near zero, then TrES-3b is best-fit with a near isothermal dayside temperature profile, along with a possible absorbing feature near 1.6 microns (Figure 2.4). These observations are disccused in Croll et al. (submitted).

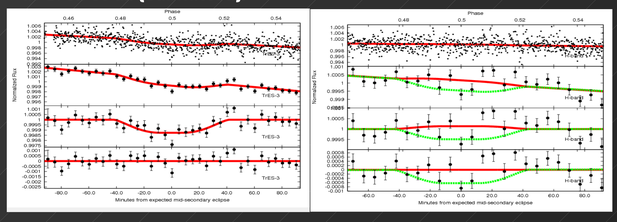

Figure 2.1: WIRCam/CFHT photometry bracketing the secondary eclipse of TrES-3b in Ks-band (left) and H-band (right). For our H-band photometry we also display the depth of the secondary eclipse that we are able to rule out at 3-sigma (green dashed-line). The format is the same as for Figure 1.1.

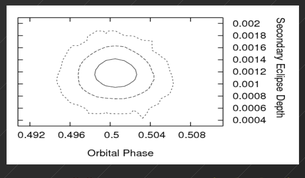

Figure 2.2: The 1-sigma (solid-line), 2-sigma dashed-line, and 3-sigma (short dashed-line) credible regions from our MCMC analysis for our Ks-band photometry showing the best-fit phase and eclipse depth.

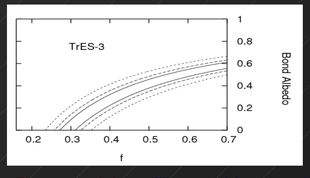

Figure 2.3: The chi-squared confidence regions on the reradiation factor, f, and Bond albedo from the combination of our Ks-band point and the Spitzer/IRAC measurements (Fressin et al. 2009. The figure is otherwise identical to Figure 1.2.

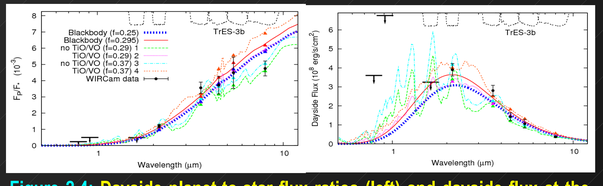

Figure 2.4: Dayside planet-to-star flux ratios (left) and dayside flux at the planet's surface (right) for TrES-3b. The Ks-band point, and H-band limit are our own. The upper-limits are from Winn et al. (2008) while the Spitzer/IRAC points are from Fressin et al. (2009). The figure is otherwise identical to Figure 1.4.

3. WASP-3b:

We detected the thermal emission of WASP-3b in Ks-band on two occasions (Figure 3.1). The two eclipses displayed similar emission to within 160 K (Figure 3.2). WASP-3b displayed very bright thermal emission (Figure 3.3).

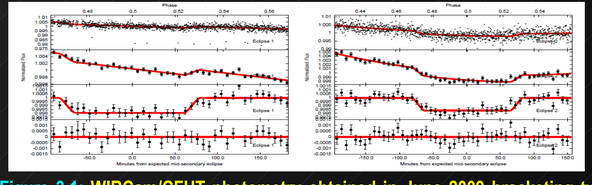

Figure 3.1: WIRCam/CFHT photometry obtained in June 2009 bracketing two Ks-band secondary eclipses of WASP-3b. The format is otherwise the same as for Figure 1.1.

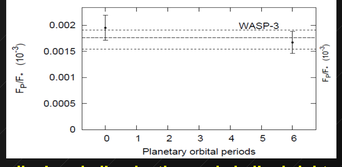

Figure 3.2: Eclipse depths of our two Ks-band eclipses. The dashed-horizontal line is the average eclipse depth from our joint analysis of our two eclipses, while the dotted-horizontal lines are the one-sigma uncertainties on this value. The two eclipses display similar depths, and similar brightness temperatures to within 160 K.

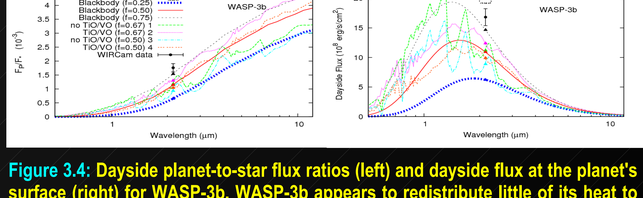

Figure 3.4: Dayside planet-to-star flux ratios (left) and dayside flux at the planet's surface (right) for WASP-3b. WASP-3b appears to redistribute little of its heat to the nightside, at least at the depth probed by our observations. The figure is otherwise identical to Figure 1.4.

4. WASP-12b:

We detected the thermal emission of WASP-12b in the Ks, H, and J-bands (Figure 4.1). The best-fit atmospheric model is displayed in Figure 4.2, while the recent possibility discussed in Campo et al. (2010) that WASP-12 has been observed to precess is constrained from the timing of our three secondary eclipses (Figure 4.3).

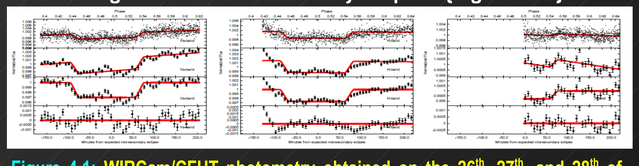

Figure 4.1: WIRCam/CFHT photometry obtained on the 26th, 27th, and 28th of December 2009 bracketing the secondary eclipse of WASP-12b in the J, H & Ks-bands, respectively. The format is otherwise the same as for Figure 1.1.

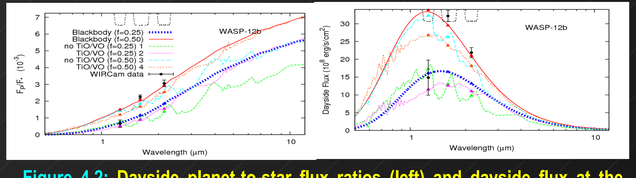

Figure 4.2: Dayside planet-to-star flux ratios (left) and dayside flux at the planet's surface (right) for WASP-12b. The atmospheric layer probed by our J-band observations appear more homogenized than layers probed by our longer wavelength observations.

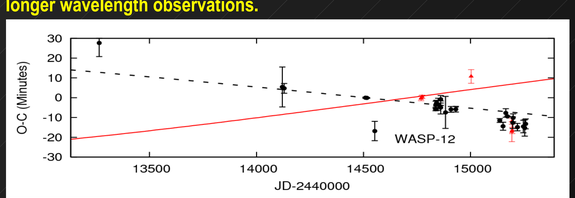

Figure 4.3: Offset (O-C) from the ephemeris for the transits (black points) and secondary eclipses (red points) for WASP-12b. The dotted black line is the expectation for the transit times, while the red solid line is the expectation for the secondary eclipse times if WASP-12b is precessing at the rate calculated by Campo et al. (2010). Our three secondary eclipses (the latest apparent single red point) do not support the precession rate suggested by Campo et al. (2010).